

Persistent entropy: a scale-invariant topological statistic for analyzing cell arrangements

N. Atienza, L. M. Escudero, M. J. Jimenez, M. Soriano-Trigueros

September 29, 2022

Abstract

In this work, we explain how to use computational topology for detecting differences in the geometrical distribution of cells forming epithelial tissues. In particular, we extract topological information from images using persistent homology and summarize it with a number called persistent entropy. This method is scale invariant, robust to noise and sensitive to global topological features of the tissue. We have found significant differences between chick neuroepithelium and epithelium of *Drosophila* wing discs in both, larva and prepupal stages.

Keywords: Topological data analysis, Persistent Entropy, Epithelial Tissues.

1 Introduction

Topology is the branch of mathematics which deals with properties of space that keep unchanged under continuous transformations. These properties are extremely important in networks. For example, distances in transit maps are usually deformed because we do not care about distances between the stops but how stops are connected.

Nowadays, computational topology and geometry are playing an increasing role in quantitative biology and biomedical engineering. In particular, the data analysis tool persistent homology [6, 21] has been successfully applied in fields such as tumor segmentation [14], analysis of biological networks [12] and diagnostic of chronic obstructive pulmonary disease [3].

Epithelia are packed tissues formed by tightly assembled cells. Their apical surfaces are similar to convex polygons forming a natural tessellation. Recently, many studies have been focused on their natural organization, in part justified because changes in this organization may indicate an early onset of disease [8, 16]. Therefore, being able to quantify differences in their topological distribution has become an interesting problem.

Due to the noisy nature of data coming from biology, this problem must be attacked statistically. Some of the statistics that capture the topological organization of the tissue are: the percentage of cells divided by number of sides [18] and the graphlet degree distribution agreement distance (GDD) [20]. Despite their achievements, both measurements relies on the local topology of the network. Therefore, a value which could be sensitive to global topological properties may offer new insights.

In particular, this statistic should be a real number for two reasons. Firstly, due to the small number of samples available for this kind of study, univariate statistical tests are the best option. Secondly, a number could be easily combined with other values in the Epigraph tool [20] to improve its classification power.

Two examples of topological statistics which are numbers and are able to measure global features of the network are persistent entropy [5, 17] and the sum of the bars in the persistence barcode (see barcode definition in section 2), which appears in [3] together with the upper star filtration under the name of branch-to-branch proximity.

In this paper, we show how persistent entropy is useful for reflecting different topological distributions in epithelial tissues. A first approach to use Topological Data Analysis for that aim was presented in

[11]. There, a weighted network was constructed to model the cell arrangements and persistent homology was computed to describe it. However, alpha complexes are known as a better model to represent a map of regions as it is the case of a segmented image of a biological tissue. For that reason, we started an experimental work in [2] using such a model and computing persistent entropy. In this paper, we improve the method, focusing in the ability of describing different topological arrangements of the cells independently of the scale of the image in terms of the number of cells involved in the sample analysed. We also further analyse statistically the experimental results to reach well-founded conclusions.

2 Methods

In this section, we describe the theoretical concepts involved in our proposal. First, we recall the tools from Topological Data Analysis used and then, how we adapt the use of these tools to the posed problem.

2.1 Topological Data Analysis concepts

Simplicial complex and filtration An n -*simplex* is the convex hull of a set of n linear independent points $\tau = \{p_1, \dots, p_n\}$. Each k -simplex contained in τ with $k < n$ is called a *face*. A *simplicial complex* \mathcal{K} (see Figure 1) is formed by a set of simplices satisfying:

1. Every face of a simplex in \mathcal{K} is also in \mathcal{K} .
2. The intersection of two simplices in \mathcal{K} is a face of both simplices.

A *filtration* over a simplicial complex \mathcal{K} is a finite increasing sequence of simplicial complexes

$$\mathcal{K}_1 \subset \mathcal{K}_2 \dots \subset \mathcal{K}_n = \mathcal{K}$$

It is commonly defined using a monotonic function $f : \mathcal{K} \rightarrow \mathbb{R}$ by which we mean that for any two simplices $\delta, \tau \in \mathcal{K}$, if δ is a face of τ , then $f(\delta) \leq f(\tau)$. That way, if $a_1 \leq \dots \leq a_n$ are the function values of all the simplices in \mathcal{K} , then the subcomplexes $\mathcal{K}_i = f^{-1}(-\infty, a_i]$, for $i = 1 \dots n$ define a filtration over \mathcal{K} .

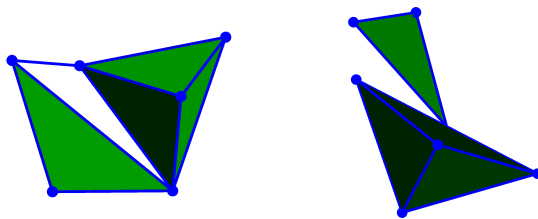


Figure 1: The picture on the left corresponds to a simplicial complex but not the one on the right.

Voronoi diagram and α -complex A *Voronoi diagram* is a partitioning of the plane depending on a set of vertices $\{v_1, \dots, v_n\}$: for each vertex v_i we define the function $d_i(x) = d(v_i, x)$ and a region given by

$$V_i = \{x \mid d_i(x) \leq d_j(x), \quad \forall j\}.$$

That is, each region is formed by points for which that vertex is the closest one (see the first image in Figure 3). An α -*complex* is a filtration [7, p. 68] that can be defined starting from a Voronoi diagram.

Consider B_r^i as the ball of center v_i and radius r . For each r , consider the region $U_r^i = B_r^i \cap V_i$ and define the simplicial complex \mathcal{K}_r with simplices

$$\tau = [v_0 \dots v_k] \in \mathcal{K}_r \Leftrightarrow \bigcap_{i=0 \dots k} U_r^i \neq \emptyset.$$

In other words, a simplex is in \mathcal{K}_r if and only if the intersection of balls with radius r and centers its vertices together with their Voronoi regions is not empty. If the points are in general position in the plane, no i -simplex will arise with i greater than 2 and the final simplicial complex is known as *Dealunay triangulation* [7, p. 63], see Figure 3.

Persistent homology and barcodes Intuitively, an n -dimensional hole in a simplicial complex is a cavity when $n = 2$, a cycle when $n = 1$ and a connected component when $n = 0$. In Algebraic Topology, the concept of *homology class* allows to define holes rigorously and compute them using linear algebra. *Persistent homology* is the main tool in Topological Data Analysis defined for tracking the persistence of holes along the filtration. For example, in the case of an α -complex constructed from a point cloud on the plane, persistent homology describes the evolution (birth, lifetime and death) of connected components and cycles as the radius of the balls increase.

The persistence of each hole is represented using intervals of the form $[a, b)$, where a is the birth time, if K_a is the simplicial complex (in the filtration) where the hole first appeared and b is the death time if K_b is the first simplicial complex (in the filtration) where the hole disappeared. If the hole remains until the final simplicial complex, we write $b = \infty$. This representation is called the *persistence barcode* and each interval a *bar*. We show an example in figure 2. A formal definition of homology and persistent homology together with fast algorithms for computing them and proofs of robustness to noise can be found in [7].

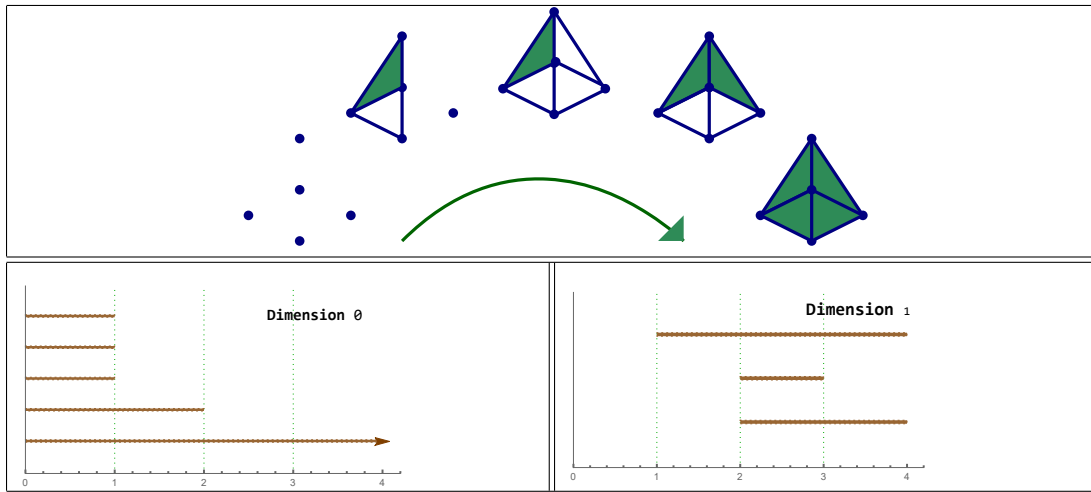


Figure 2: Top: example of a filtration \mathcal{K} . Bottom: barcodes representing connected components and cycles.

Persistent entropy Barcodes are very intuitive but their statistical analysis is rather complex [13]. Landscapes are an equivalent representation which are more suitable for it, but statistics on them lack of specific tests so far and rely on the law of large numbers [4]. Therefore, in order to perform a useful statistical analysis of persistent homology for small samples, we need a real number that encapsulates the information contained in the barcode. *Persistent entropy* is a stable topological statistic [1] and can be seen as an adaptation of Shannon entropy (Shannon index in ecology) to the persistent homology context.

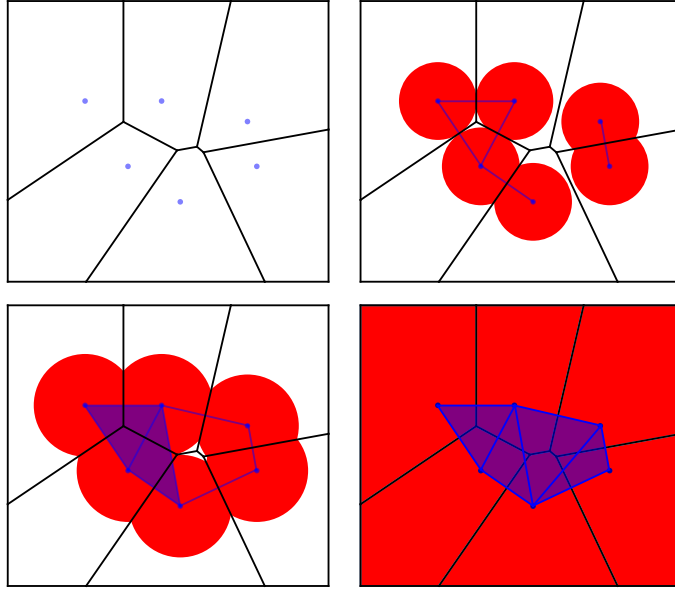


Figure 3: An example of alpha complex filtration. The first image coincide with the Voronoi diagram and the last one with the Dealunay triangulation

Given a barcode without infinite bars $B = \{[a_i, b_i]\}_{i=1\dots n}$ consider the length of the bars $\ell_i = b_i - a_i$ and their sum $L(B) = \ell_1 + \dots + \ell_n$. Then, its *persistent entropy* is:

$$E(B) = \sum_{i=1}^n -\frac{\ell_i}{L(B)} \log\left(\frac{\ell_i}{L(B)}\right)$$

Note that we are normalizing lengths of the bars for calculating persistent entropy. In addition, $L(B)$ may be used, as well, as a statistic, in case that such a normalization is not desirable.

2.2 The normalization and scale invariance problems

The common workflow when using persistent homology consists in taking the data, defining a filtration over it and computing its persistent homology and associated barcode. For this study, we will consider the centroids of the cells in each image, use the Voronoi diagram to approximate the cells boundary and compute its α -complex. After that, we would analyze their barcodes statistically using persistent entropy. Persistent entropy is very sensitive to the number of bars appearing in the barcode and, hence, to the number of cells as well. If we want to be sure we are finding differences in the topological distribution and not in the number of cells appearing in the image, we have to make a normalization. Using that the maximum entropy for a barcode of n bars is $\log(n)$, we could normalize dividing by that value, $E(B)/\log(n)$, obtaining a value between 0 and 1. Unfortunately, apart from loosing the stability properties [1], the variance of $E(B)/\log(n)$ seems to depend on n and therefore the number of bars still affects to the statistical study. For this reason, it is convenient to make an a priori normalization: on the number of cells that appear in the image. If all the images have the same number of cells, then the 0-dimensional persistence barcode will have the same number of bars (one per cell). Notice that, while having the same number of cells, there may be differences in the number of cycles (1-dimensional persistent homology) but this is good, since it represents differences in the topological distribution.

In addition, we expect this method to be scale invariant. Otherwise, the result may vary from images of one tissue to other even if they have the same topological distribution.

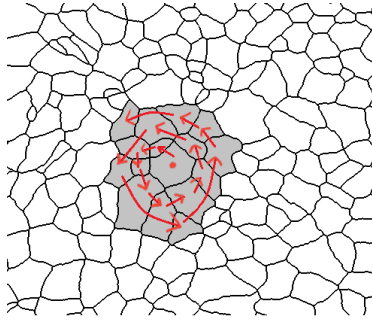


Figure 4: Intuition behind the algorithm. We pick cells following a spiral until the desired number is reached.

Normalization of number of cells In order to minimize the addition of fake cycles in the process of normalization of the number of cells, we select the cells to be processed following a spiral like in Figure 4. Note that this process is expected to work well due to the convexity of the cells. We detail the process in Algorithm 1. Our input is a gray scale image M , where pixels corresponding to each region (cell) are labelled with the same number and the boundaries of those regions are set to 0. Figure 5 shows a simple example in which, taking as input $n = 5$ and the depicted pixel values, the output of the algorithm is the set of cells with labels $\mathcal{C} = \{4, 3, 5, 2, 7\}$.

Scale invariance of the method Persistent entropy makes use of normalized lengths of bars in the barcode and, hence, it is invariant to changes of scale in the image. Besides, persistent entropy is only defined for finite bars but we may be interested in barcodes with infinite bars. In that case, what is commonly done is to limit these bars to a big enough value in the filtration or eliminate them, depending on how important infinite bars are considered with respect to others. In our case, as α -complex always have one connected component and no cycles for a radius big enough, there is only one infinity bar. This 0-dimensional bar always exists and is born at moment 0 so gives no information about the topology of the cells arrangement and we can remove it. Actually, if we do not remove it but limit its endpoint to a fixed value, we eliminate the scale invariance of the method since the same pattern, once re-scaled, will have a different barcode as shown in Figure 6.

Therefore, we have removed the infinity bar of all barcodes in this experiment. This is the main improvement with respect to the communication [2] and the differences in results are analyzed in Section 3.2.

3 Example and computational experiments

In order to obtain the persistent entropy of each image, we use the techniques explained in the previous section as displayed in Figure 7. Basically, we take a fixed number of cells from each image, obtain their centroids and compute their α -complex. Use this filtration to compute persistent homology and remove the infinite bar to calculate persistent entropies of 0-dimensional and 1-dimensional persistence barcodes respectively.

Example Before doing the experiment with cell tissues, we want to test it in a simpler situation. A common model for epithelial tissues is given by a sequence of images called CVT path [19]. The first image in the sequence is constructed by producing a fixed number of random points and computing its Voronoi diagram. The rest of the images in the sequence are obtained from the previous one by taking the centroids of the Voronoi cells and computing its Voronoi diagram again (note that the point generating a Voronoi cell is usually not its centroid). We will use persistent entropy to experimentally separate the first and fifth images of CVT paths, which are expected to have quite different topological distributions, as seen in Figure 8.

Algorithm 1 Spiral normalization of regions

```

1: procedure SPIRAL( $M, n$ )
2:    $\mathcal{C} := \emptyset$ 
3:    $(x, y) := \text{center}(M)$ 
4:   if  $M(x, y) \neq 0$  then
5:      $\mathcal{C} := \{M(x, y)\}$ 
6:   end if
7:    $i := 0$ 
8:   while  $\mathcal{C} < n$  do
9:      $i := i + 1$ 
10:    for  $j \in (0, \dots, i + 1)$  do
11:      if  $\#\mathcal{C} < n$  then
12:         $y := y + (-1)^{i+1}$ 
13:        if  $M(x, y) \neq 0$  and  $M(x, y) \notin \mathcal{C}$  then
14:           $\mathcal{C} := \mathcal{C} \cup \{M(x, y)\}$ 
15:        end if
16:      end if
17:    end for
18:    for  $j \in (0, \dots, i + 1)$  do
19:      if  $\#\mathcal{C} < n$  then
20:         $x := x + (-1)^{i+1}$ 
21:        if  $M(x, y) \neq 0$  and  $M(x, y) \notin \mathcal{C}$  then
22:           $\mathcal{C} := \mathcal{C} \cup \{M(x, y)\}$ 
23:        end if
24:      end if
25:    end for
26:  end while
27:  return  $\mathcal{C}$ 
28: end procedure

```

$\triangleright M$ is an image and n a number
 \triangleright central coordinates of M
 \triangleright repeat $i + 1$ times
 $\triangleright \#$ means number of elements
 \triangleright repeat $i + 1$ times
 \triangleright return the first n regions around the center

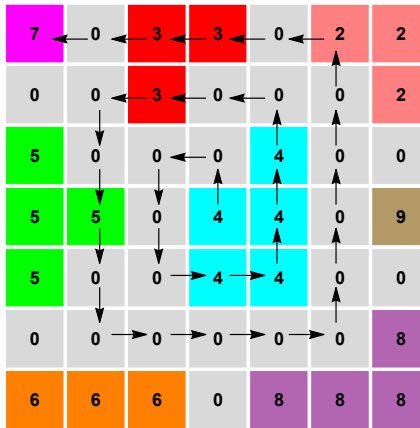


Figure 5: Example of how the algorithm works at pixel level.

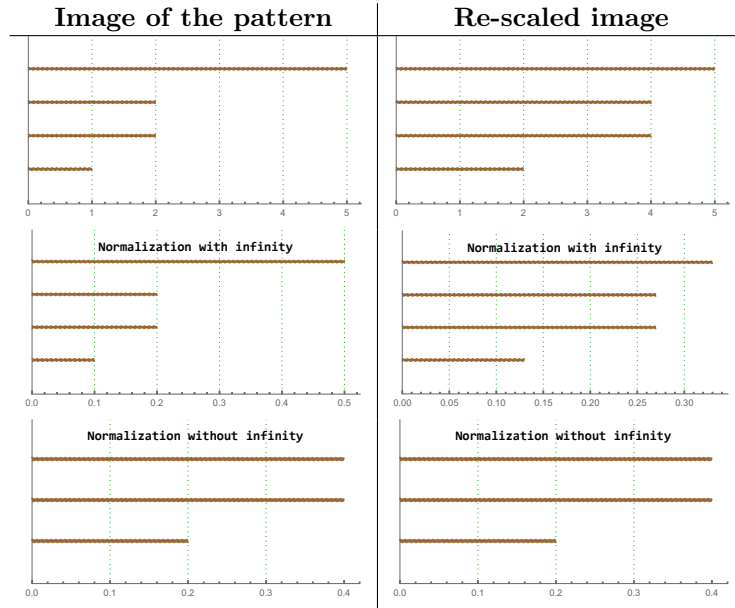


Figure 6: The top barcodes are calculated from images with the same pattern differing with a scalar factor of two. The infinite bar have been limited to 5. In the second row, the normalization produce different barcodes. The third row shows how normalizing barcodes after removing the infinity bar provides the same barcodes.

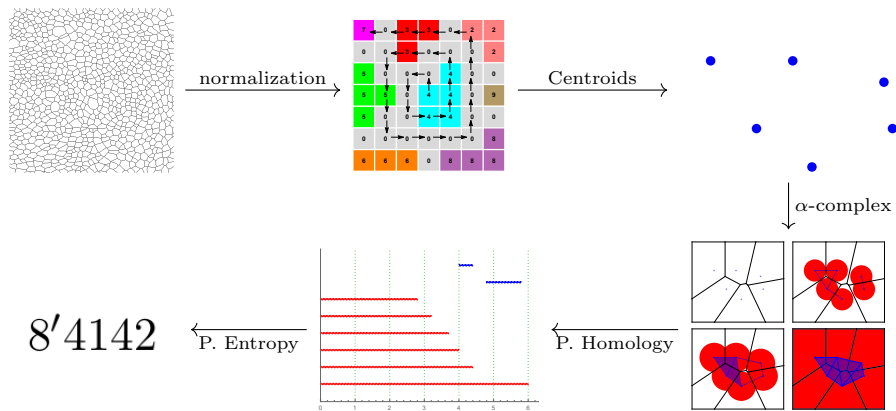


Figure 7: Diagrams with the steps followed to obtain the persistent entropy values. It can be calculated for both, 0 dimensional bars (the red bars in the barcode) and 1 dimensional bars (the blue ones).

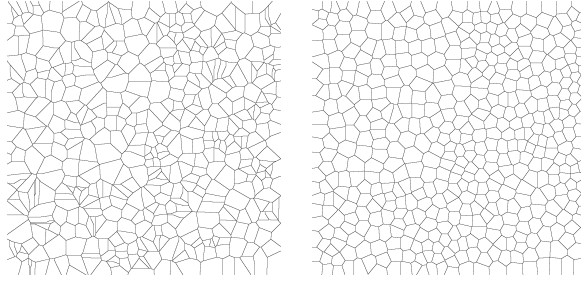


Figure 8: The first and fifth image of a CVT path

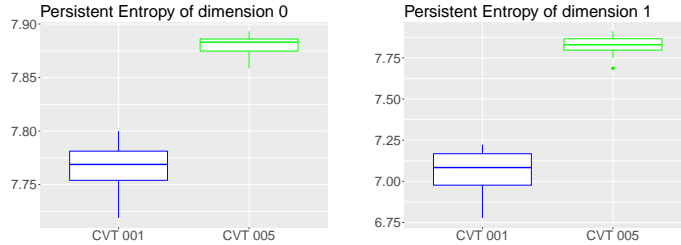


Figure 9: Results for the first and fifth images of CVT paths. Note that the two groups are perfectly separated.

We have taken a sample of 20 CVT paths and taken 250 cells from its first and fifth images. Then, we have calculated their persistent entropy of 0-dimensional and 1-dimensional persistence barcodes. Both types of images were clearly distinguished by our method as shown in Figure 9.

3.1 Epithelial tissues

Images used in the main experiment are from three different epithelial tissues: chick neuroepithelium (cNT), wing disc in the larva (dWL) and prepupal stages (dWP) from *Drosophila*, see Figure 10. The first one is clearly different to the other two so we should be able to find differences in their topological distribution. The other two tissues are taken from two proliferative stages separated by 24 hours of development, and topological differences (if they exist) are expected to be very difficult to prove. Further information about the way images were obtained and segmented can be found in [9]. The data base consists of 16 images of cNT, 16 of dWP and 15 of dWL. Table 1 shows their number of valid cells (cells which do not intersect with the boundary of the image). We fix 245 for the normalization of number of cells and perform the process described in Figure 7, obtaining two persistent entropy values for each of

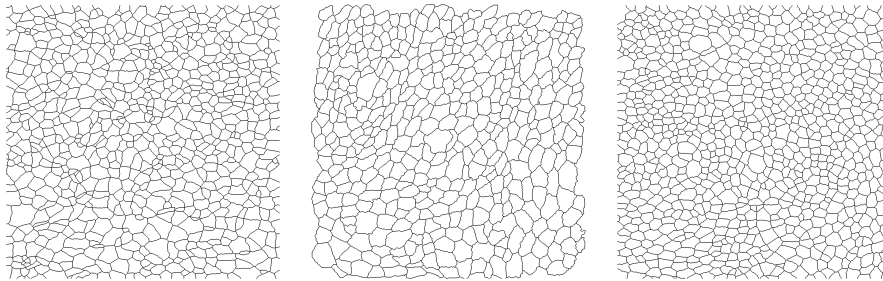


Figure 10: Image of tissues coming from cNT, dWL and dWP.

Table 1: The number of cells in each picture.

	1	2	3	4	5	6	7	8	9	10	11	12	13	14	15	16
cNT	666	661	565	573	669	532	419	592	743	527	594	473	704	747	469	834
dWP	748	805	566	414	454	654	751	713	503	430	387	516	413	455	271	249
dWL	426	555	491	522	510	936	890	789	977	913	604	835	785	747	622	

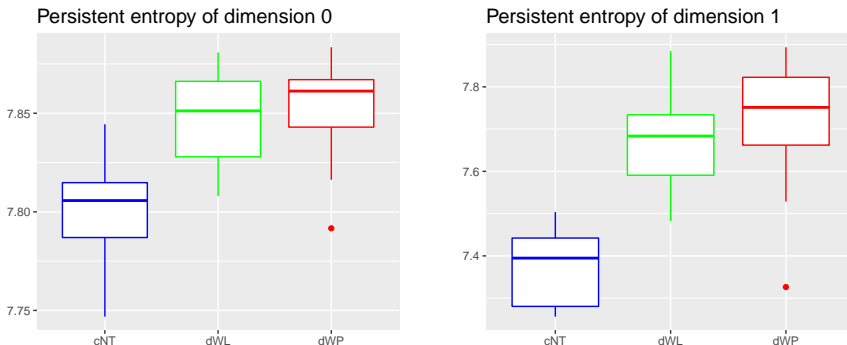


Figure 11: Boxplot representation of persistent entropy for the zero and first persistent homology of the three tissues.

the images. We represent this information in Figure 11, note that cNT values differ clearly with respect to the other two classes. We have performed a Kruskal-Wallis Test to see if there are significant differences between the persistent entropy of the tissues. When we obtain a p -value smaller than 0.05, we consider there are significant differences between their persistent entropy, and therefore between their topological distribution. If this condition is satisfied, we can perform a Dunn Test to see if there are significant differences pairwise. Results are shown in Table 2. We have found significant differences between cNT and $\{dWP, dWL\}$, but not between these last two.

In order to have a richer view, we repeat the experiment changing the number of cells we take in each image, $n = 5, 10, 15, \dots, 385$ and calculate their p -values, see Figure 12. The last two images of dWP have too few cells, so we remove them from these experiments (the results for $n < 245$ are barely the same without them). As we can see, the topological differences in the network are found quite soon, it is usually enough with 10-30 cells, except for dWL vs dWP which is barely always quite far from the significance level.

3.2 Comparison with previous method

The method explained in this paper differs from [2] in how the infinity bar of the connected component is treated. As we have reasoned in 2.2, limiting the infinity bar to a fixed value may affect to the scale

Table 2: Kruskal-Wallis Test and Dunn Test for comparing the persistent entropies of the processed tissue images.

KWT	PE_0	PE_1
p-value	1.846e-05	7.731e-07

DT p-value adjusted	dWL vs dWP	cNT vs dWL	dWP vs cNT
PE_0	0.6528346	3.560990e-04	5.930129e-05
PE_1	0.3764610	1.144703e-04	1.816071e-06

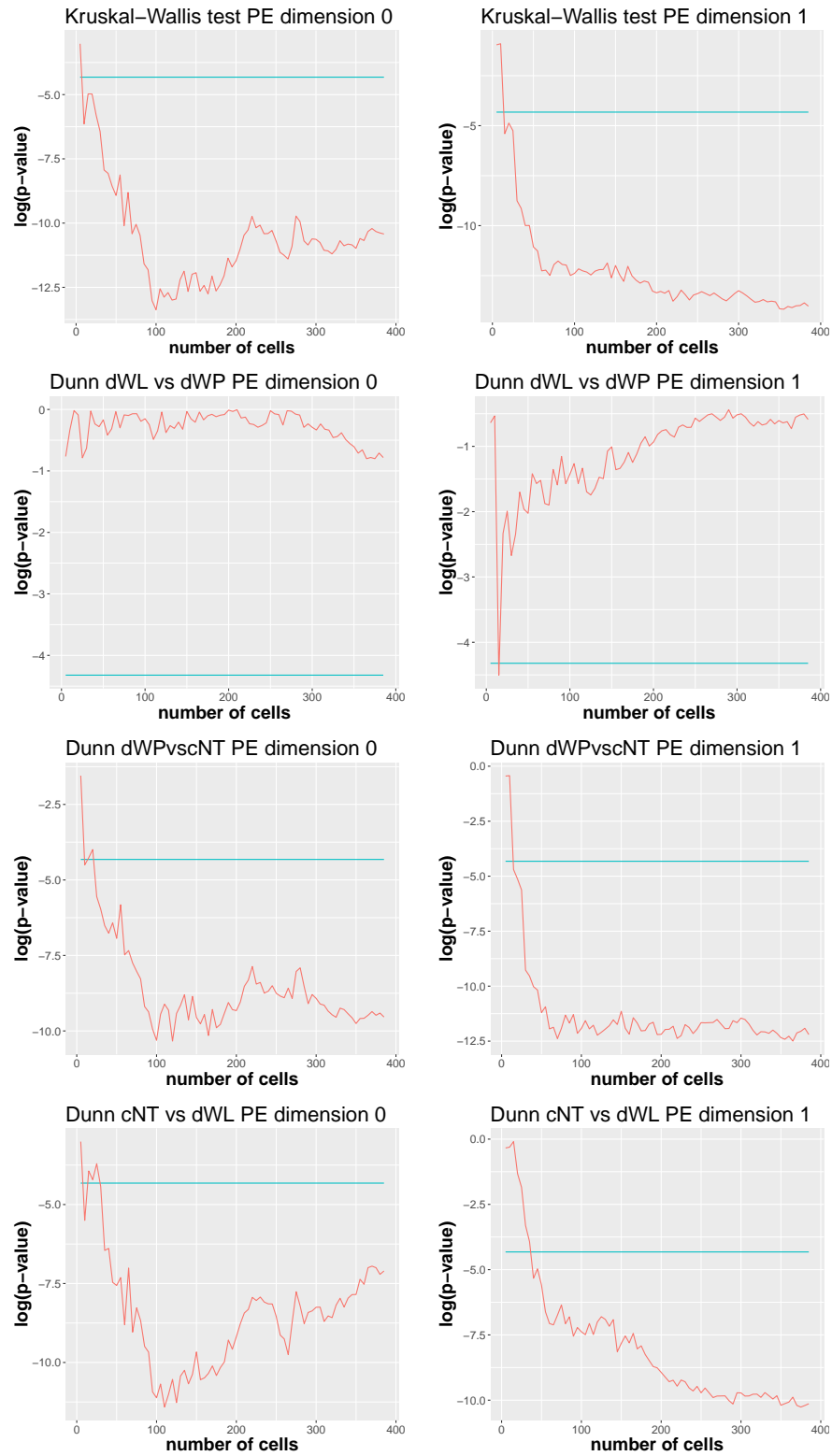


Figure 12: Results of the statistical tests for each n . The y value of the plot is the logarithm of the p -values. The vertical line represent the logarithm of the significance level 0.05.

Table 3: Dunn Test results when the infinity bar is not eliminated

DT p-value adjusted	dWL vs dWP	cNT vs dWL	dWP vs cNT
PE_0	0.02671554	0.01600541	7.574294e-06
PE_1	0.3271768	5.791831e-05	2.162007e-06

Table 4: Dunn Test for the sum of the length

DT p-value adjusted	dWL vs dWP	cNT vs dWL	dWP vs cNT
PE_0	0.009794481	0.233509505	0.150413416

invariance of entropy. However, in the communication [2] we kept the infinity bar, considering its length to be 2500, which is the maximum of all filtrations functions determining the α -complexes. This affected the scale invariance of the method, and therefore the size of the image changed the value of persistent entropy. In that experiment, the p-values of Kruskal-Wallis Test for both, 0 and 1 dimensional persistent entropy, were under 0.05. As it can be seen in Table 3, the 0 dimensional p -value of dWL vs dWP is much smaller than the obtained when removing the infinite bar. This fact suggests big differences of scales between images of dWL and dWP while no significant differences in their topological distribution were found. Therefore, if we use a statistic sensitive to scale, like the sum of the lengths $L(B)$, we should find significant differences between them. This is exactly the case, the p -value of the Kruskal-Wallis test is 0.01228 and the Dunn Test result can be seen in Table 4. Note that, in this case, the test do not find significant differences between cNT and the other two since its scale is somewhere between the ones of dWP and dWL.

3.3 Implementation

All functions used for these computational experiments can be found in <https://github.com/Cimagroup>. The software used are the following:

- Matlab: image regions were obtained using regionprops function and the spiral algorithm has been implemented for this tool.
- R: The α -complexes, persistent homology and barcodes were computed using the TDA package [10]. We have written functions for calculating persistent entropy and the sum of the lengths. The statistical tests used are from the FSA package [15].

4 Conclusions

We have used persistent entropy to find differences between the topology of the epithelium cNT and the topologies of both, dWL and dWP. This method is robust to noise, scale invariant and sensitive to global properties of the network, making it a great statistic for summarizing the topology of any region-based segmented image.

In particular, this technique open the door to perform non-parametric tests for rejecting when two biological structures have the same topological distribution. This kind of tests are the best for samples with a small amount of data, which is usually the case for these kind of studies. We hope this technique may help to improve existing topological tools for tissues, such as [20].

This procedure could be easily generalized to 3D tissues formed by convex cells. In order to extend it to non convex-cells or any other kind of networks, a different filtration (probably not the one provided by α -complexes) should be defined.

References

- [1] Atienza, N., Gonzalez-Diaz, R., Soriano-Trigueros, M. On the stability of persistent entropy and new summary functions for TDA. arxiv/1803.08304, 2018.
- [2] N. Atienza, L.M. Escudero, M.J. Jimenez, M. Soriano-Trigueros. Characterising epithelial tissues using persistent entropy. In: R. Marfil, M. Caldern, F. Daz del Ro, P. Real, A. Bandera. Computational Topology in Image Context. 7th International Workshop, CTIC 2019. Proceedings LNCS, volume 11382, 2019.
- [3] J. Brodzki, K. Belchi, R. Djukanovic, J. Conway, M. Pirashvili, M. Bennett. Lung Topology Characteristics in patients with Chronic Obstructive Pulmonary Disease. Scientific Reports. 8. 10.1038/s41598-018-23424-0. 2018.
- [4] P. Bubenik. Statistical Topological Data Analysis using Persistence Landscapes. Journal of Machine Learning Research 16, 77-102, 2015.
- [5] H. Chintakunta, T. Gentimis, R. Gonzalez-Diaz, M. J. Jimenez, H. Krim. An entropy based persistence barcode. Pattern Recognition, 48-2, pages 391-401, 2015.
- [6] H. Edelsbrunner, D. Letscher, A. Zomorodian. Topological persistence and simplification. FOCS '00, IEEE Computer Society, 454-463, 2000.
- [7] H. Edelsbrunner, J.L. Harer. Computational Topology: An Introduction. American Mathematical Society, 2010.
- [8] V. Emmanuele, A. Kubota, B. Garcia-Diaz, C. Garone, H.O. Akman, D. Snchez-Gutierrez, L.M. Escudero, S. Kariya, S. Homma, K. Tanji et al. Fhl1 W122S causes loss of protein function and late-onset mild myopathy. Hum. Mol. Genet.24. 2015.
- [9] L.M. Escudero, L.F. Costa , A. Kicheva, J. Briscoe, M. Freeman, M.M. Babu. Epithelial organisation revealed by a network of cellular contacts. Nat Commun. 2011;2:526. doi:10.1038/ncomms1536. 2011.
- [10] B.T. Fasy, J. Kim, F. Lecci, C. Maria, V. Rouvreau. The included GUDHI is authored by Maria, C. and Dionysus by Morozov, D. and PHAT by Bauer, U., Kerber, M., Reininghaus, J. TDA: Statistical Tools for Topological Data Analysis. <https://CRAN.R-project.org/package=TDA>. R package version 1.6. 2017.
- [11] M.J. Jimenez, M. Rucco M, P. Vicente-Munuera, P. Gmez-Glvez, L.M. Escudero. Topological Data Analysis for Self-organization of Biological Tissues. In: Brimkov V., Barneva R. (eds) Combinatorial Image Analysis. IWCIA 2017. Lecture Notes in Computer Science, 10256, 229-242, 2017.
- [12] E. Merelli, M. Rucco, P. Sloot, L. Tesei. Topological Characterization of Complex Systems: Using Persistent Entropy. Entropy 2015, 17(10), 6872-6892; doi:10.3390/e17106872. 2015.
- [13] Y. Mileyko, S. Mukherjee, J. Harer. Probability measures on the space of persistence diagrams. Inverse Problems 27(12), 2011.
- [14] T. Qaiser, Y-W. Tsang, D. Taniyama, N. Sakamoto, K. Nakane, D. Epstein, N. Rajpoot. Fast and Accurate Tumor Segmentation of Histology Images using Persistent Homology and Deep Convolutional Features. arXiv:1805.03699, 2018.
- [15] D.H. Ogle, P. Wheeler, A. Dinno. FSA: Fisheries Stock Analysis. R package version 0.8.22, <https://github.com/droglenc/FSA>. 2018.
- [16] J.A. Park, J.H. Kim, D. Bi, J.A. Mitchel, NT. Qazvini, K. Tantisira, C.Y. Park, M. McGill, S.H. Kim, B. Gweon et al. Unjamming and cell shape in the asthmatic airway epithelium. Nat. Mater.14, 10401048. 2015.

- [17] M. Rucco, F. Castiglione, E. Merelli, M. Pettini. Characterisation of the Idiotypic Immune Network Through Persistent Entropy. Proceedings of ECCS 2014. Springer Proceedings in Complexity, pages 117-128, 2014.
- [18] D. Sanchez-Gutierrez, A. Saez, A. Pascual, L.M. Escudero. Topological progression in proliferating epithelia is driven by a unique variation in polygon distribution. PLoS One8, e79227. 2013.
- [19] D. Sanchez-Gutierrez, M. Tozluoglu, J.D. Barry, A. Pascual, Y. Mao, L.M. Escudero, Fundamental physical cellular constraints drive self-organization of tissues. The EMBO Journal volume 35, number 1, pages 77-88, 2016.
- [20] P. Vicente-Munuera, P. Gomez-Galvez, A. Tagua, M. Letran, Y. Mao, L.M. Escudero. EpiGraph: an open-source platform to quantify epithelial organization. BioRxiv 217521; 10.1101/217521. 2018.
- [21] A. Zomorodian, G. Carlsson: Computing persistent homology. Discrete and Computational Geometry 33 (2), 249-274, 2005.